Evaluation of bone impingement prediction in pre-operative planning for shoulder arthroplasty

P R Krekel, P W de Bruin, E R Valstar, F H Post, P M Rozing and C P Botha

Proceedings of the Institution of Mechanical Engineers, Part H: Journal of Engineering in Medicine 2009 223: 813
DOI: 10.1243/09544119JEIM531

Evaluation of bone impingement prediction in pre-operative planning for shoulder arthroplasty

P R Krekel[1,2*], **P W de Bruin**[3], **E R Valstar**[1,4], **F H Post**[2], **P M Rozing**[1], and **C P Botha**[2,3]
[1]Department of Orthopaedics, Leiden University Medical Center, Leiden, The Netherlands
[2]Data Visualisation Group, Delft University of Technology, Delft, The Netherlands
[3]Department of Radiology, Leiden University Medical Center, Leiden, The Netherlands
[4]Department of Biomechanical Engineering, Delft University of Technology, Delft, The Netherlands

The manuscript was received on 14 October 2008 and was accepted after revision for publication on 19 December 2008.

DOI: 10.1243/09544119JEIM531

Abstract: In shoulder arthroplasty, malpositioning of prostheses often leads to reduced post-operative range of motion (ROM) and complications such as impingement, loosening, and dislocation. Furthermore, the risk of impingement complications increases when reverse total prostheses are used. For this purpose a pre-operative planning system was developed that enables surgeons to perform a virtual shoulder replacement procedure. The present authors' pre-operative planning system simulates patient-specific bone-determined ROM meant to reduce the risk of impingement complications and to improve the ROM of patients undergoing shoulder replacement surgery. This paper describes a validation experiment with the purpose of ratifying the clinical applicability and usefulness of the ROM simulation module for shoulder replacement surgery.

The experiment was performed on cadaveric shoulders. A data connection was set up between the software environment and an existing intra-operative guidance system to track the relative positions of the bones. This allowed the patient-specific surface models to be visualized within the software for the position and alignment of the tracked bones. For both shoulders, ROM measurements were recorded and tagged with relevant information such as the type of prosthesis and the type of movement that was performed. The observed ROM and occurrences of impingement were compared with the simulated equivalents. The median deviation between observed impingement angles and simulated impingement angles was -0.30° with an interquartile range of 5.20° (from -3.40° to 1.80°). It was concluded that the ROM simulator is sufficiently accurate to fulfil its role as a supportive instrument for orthopaedic surgeons during shoulder replacement surgery.

Keywords: medical visualization, pre-operative planning, shoulder, arthroplasty, range of motion, motion tracking

1 INTRODUCTION

Shoulder arthroplasty (Fig. 1) aims to provide pain relief and to restore joint mobility. However, success rates in shoulder replacements are considerably lower than in knee and hip replacements [**1**]. This can be partially ascribed to the complexity of the shoulder joint. The surgical exposure provides little room for manoeuvring the instruments and causes the field of view for the surgeon to be limited. This frequently results in malalignment of prostheses [**2**]. Malalignment of shoulder prostheses leads to a diverse range of complications, e.g. increased wear, reduced stability of the glenohumeral joint, limited range of motion (ROM), and impingement [**3**, **4**]. Long-term consequences of impingement are abrasion of bone, loosening of the prosthesis, and increased risk for the necessity of revision surgery [**5**].

*Corresponding author: Department of Orthopaedics, Leiden University Medical Center, Albinusdreef 2, Leiden, 2333ZA, The Netherlands.
email: P.R.Krekel@lumc.nl

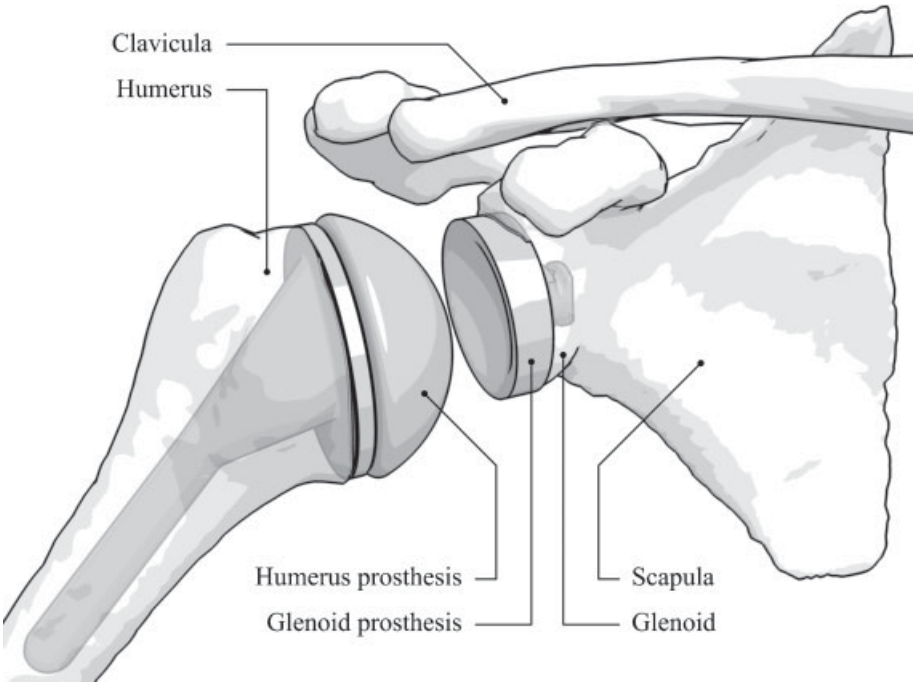

Fig. 1 Illustration of a shoulder joint after total shoulder replacement

Impingement complications are frequently seen with reverse shoulder prostheses, a type of prosthesis usually indicated for patients who suffer from a severely impaired rotator cuff [**6–8**]. Scapular notching refers to impingement of the humeral cup with the glenoid neck and is the type of impingement that is most common for reverse shoulder prostheses. Sirveaux *et al.* [**9**] carried out a multi-centre study consisting of 80 shoulders, which showed scapular notching in 51 cases. A similar study by Juvenspan *et al.* [**10**] showed scapular notching in 39 of 55 cases. Conversely, several studies show that careful planning greatly reduces the risk on scapular notching [**11–13**].

Anticipating the frequent occurrence of impingement and the clear need to prevent it, a pre-operative planning system for shoulder replacements that interactively simulates bone-determined ROM was developed. The system was described in detail in a previous publication [**14**]. A short summary of the system is included in section 2.1.

This paper describes an experiment for the validation of the ROM simulations. The purpose of the experiment was to determine the accuracy of the ROM simulator. In addition, the ability of the system to predict impingement complications such as scapular notching was evaluated. The prediction of bone impingement enables the surgeon to set up a plan that explicitly avoids this type of complication.

2 METHODS

2.1 Description of the pre-operative planning system

The pre-operative planning system loads computed tomography (CT) data and extracts surface models of the scapula and humerus. Subsequently, the surgeon can place prosthesis models on the bone models. Currently, the system only supports total glenohumeral prostheses, i.e. both a cup and a ball component have to be placed. The system does support total reverse prostheses.

The system automatically calculates the position of well-known landmarks on the bone models. Planes are moved through the object to find the most extreme points on the models. The centre of rotation of the glenoid is determined by applying a Hough transform to the surface models. The landmarks can also be selected manually. Using the landmark positions, a predefined pre-operative plan is transformed to the patient-specific case. Subsequently, prostheses can be dragged to different positons, thereby altering the plan.

In order to calculate the ROM, a biomechanical model of the glenohumeral joint was implemented. A generally accepted hypothesis is that the glenohumeral joint can be approximated by a ball joint [**15**, **16**]. No displacement is taken into account. The scapula coordinate system as described in the recommen-

dations of the International Society of Biomechanics [**17**] was used. The coordinate system is depicted in Fig. 2. In this paper, clinical terms are used to describe motion. Anteflexion refers to elevation parallel to the sagittal plane along the Z axis, abduction refers to elevation in the coronal plane along the X axis, and endorotation refers to axial rotation along the humeral shaft or Y axis.

Bone-determined ROM is automatically determined by systematically reorienting the humerus with a placed humeral component in all directions, starting from an initial abduction of 45°, while checking for collisions with a collision detection algorithm [**18**]. During alterations of a pre-operative plan, the ROM is continuously being calculated and visualized with a specialised visualization technique (Fig. 3). If the ROM in a certain direction deteriorates, this is depicted with red surfaces. If it improves, this is depicted with green surfaces. This provides an intuitive user interface for the surgeon to optimize a plan with regards to the ROM. Automatic optimization is not yet incorporated, mainly because the ROM is not the only aspect that plays a part in determining the most optimal alignment. For instance, fixation of the prosthesis is optimal when the screws are inserted through thick cortical bone. Also, the orientation of the components determines the post-operative stability of the joint [**3**].

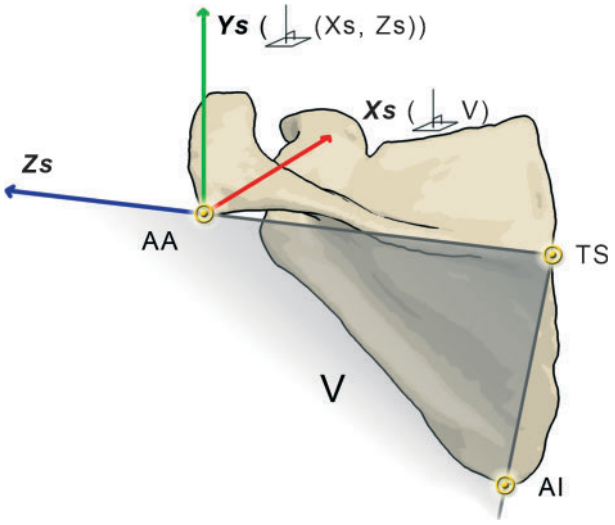

Fig. 2 Definition of the scapula coordinate system: AA, angulus acromialis; TS, trigonum spinae scapulae; AI, angulus inferior; Os, the origin coincident with AA; Z_s, the line connecting TS and AA, pointing to AA; X_s, the line perpendicular to the plane formed by AI, AA, and TS, pointing forwards; Y_s, the common line perpendicular to the X_s and Z_s axes, pointing upwards

Future work includes the implementation of an intra-operative guidance system, enabling the surgeon to carry out the operation in accordance with the pre-operative plan.

2.2 Validation experiment

The outline of the experiment is depicted in Fig. 4. For this experiment the intact shoulders of a cadaver were used. The cadaver had been specially embalmed to maintain flexibility of the extremities (Complucad ANATOMIC, Complucad International S.A.).

First, a series of axial CT scans was made using clinical shoulder protocols (Toshiba Aquilion CT Scanner, Toshiba Medical Systems, Otawara, Japan). The scan data were reconstructed at $512 \times 512 \times 541$ voxels, with spatial dimensions of $0.54\,\text{mm} \times 0.54\,\text{mm} \times 1.0\,\text{mm}$. The CT scans of both shoulders

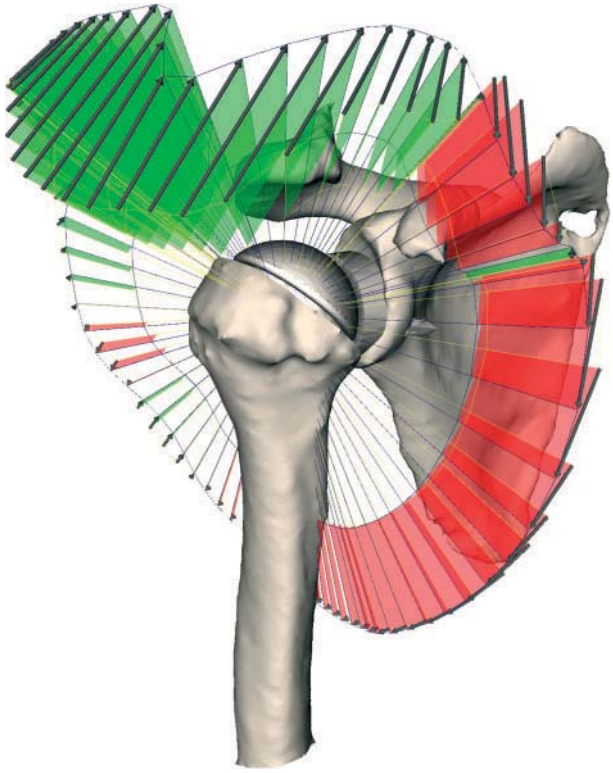

Fig. 3 A screenshot of the ROM simulator, showing the difference between two shoulder replacement plannings. While the surgeon alters the planning, the visualization changes. Green (left of the figure) surfaces denote that the ROM is improving with respect to the previous planning, while red (right of the figure) surfaces denote that the ROM is deteriorating. This allows the surgeon to optimize the planning with regard to the ROM

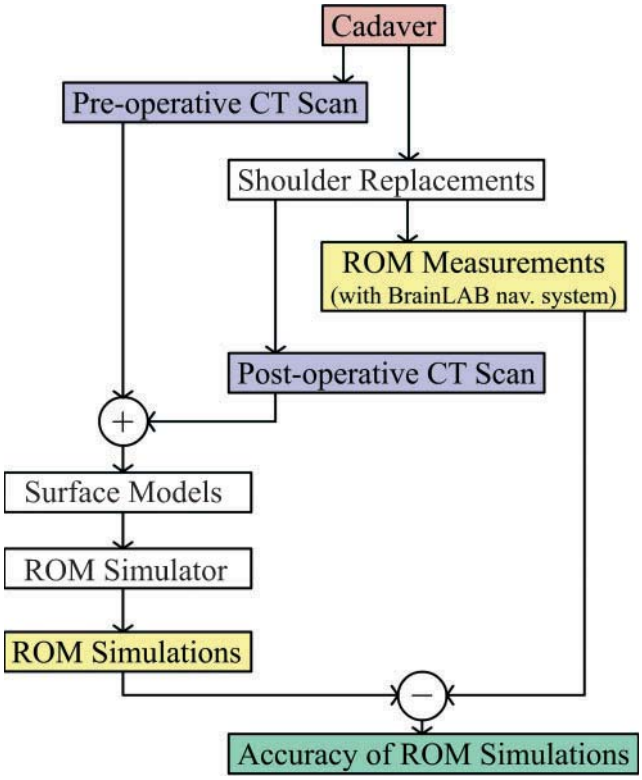

Fig. 4 This diagram shows the outline of the validation experiment. First, a pre-operative CT scan was made. Shoulder replacements were performed on both shoulders. A post-operative CT scan was made and these data were combined with the pre-operative plan to repair faults as a result of scattering caused by the prostheses. These data were converted to surface models and used for ROM simulations. ROM measurements were also performed on the cadaver with an optical tracking system. These observations were compared with the ROM estimations from the ROM simulator

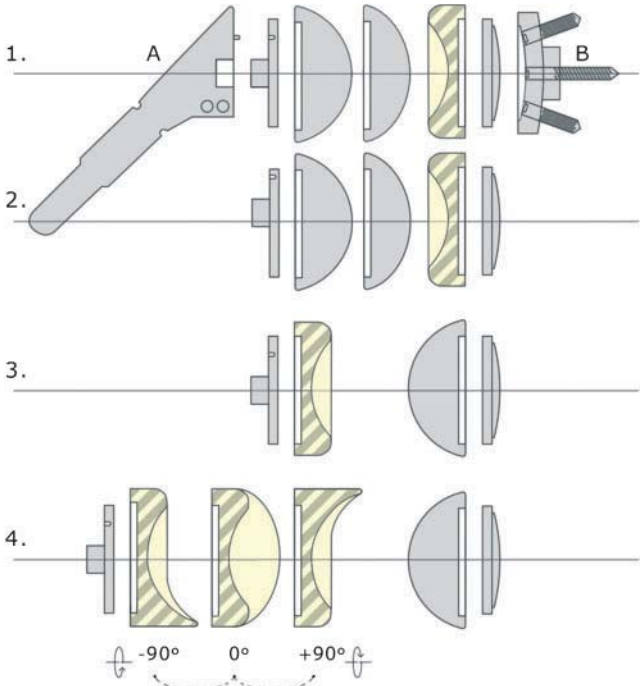

Fig. 5 An overview of the modular ESKA Multiplex shoulder prosthesis. A is the humeral base component, with detachable stem. B is the glenoid base component. Lines 1 to 4 show the different configurations used during the experiment: line 1, a normal total shoulder prosthesis with an 18 mm spherical head; line 2, a normal total shoulder prosthesis with excentric humeral components with 14 mm and 18 mm spherical heads; line 3, a reversed total shoulder prosthesis; line 4, a reversed total shoulder prosthesis with three orientations of a polyethylene cup with a slope for the humeral side

were segmented using the DeVIDE visualization platform [**19**]. Following segmentation, surface models of the scapulae and humeri were created.

Shoulder replacement procedures were performed on both shoulders of the cadaver. The modular ESKA Multiplex shoulder prosthesis (ESKA Implants GmbH & Co, Lübeck, Germany) was used, which consists of two base platforms for the scapula and the humerus. The prosthesis can be tailor fitted to the patient using different components that are attached to the base platforms (Fig. 5). This allows multiple configurations of types (normal and reversed) and sizes to be analysed, just as the pre-operative planning environment allows for quick interchanging of prostheses. To vary the set of impingement angles, the base platform of the left humerus was deliberately positioned with a different inclination and more distally than the base platform of the right shoulder.

A computer navigation system (BrainLAB VectorVision, BrainLAB AG, München, Germany) was used for real-time tracking of shoulder motion. The navigation system uses two infrared cameras and retroreflective markers on the instruments and marker trees. This system is used in the authors' hospital for various orthopaedic surgery procedures (spine, knee, and hip replacements). At the time of writing, no shoulder-specific module was available. To enable motion tracking of the shoulder bones, basic registration and tracking functionality was implemented as described below. Communication with the navigation system was accomplished by using a research software library (VectorVision Link, BrainLAB AG, München, Germany).

A marker tree consists of three retroreflective markers that are attached to a metal Y- or T-frame.

Different configurations of the markers allow the navigation system to identify specific marker trees and instruments. The marker trees are attached to guidewires with a diameter of 3 mm, which are drilled into the bone. This fixation is important, because any relative movement between the marker tree and the bone will be misinterpreted as movement of the bone.

After fixation, the surgeon registers each marker tree to its corresponding bone (Fig. 6). Using a sharp pointer device with retroreflective markers, a number of specific landmarks are indicated on the bone. The same landmarks are indicated in the intra-operative planning module, after which the registration matrix can be calculated.

The marker tree that is attached to the scapula is used as the reference coordinate system. The pointing device and the marker tree attached to the humerus report their position and orientation in this coordinate system. After registration of the scapula and the humerus, the intra-operative tracking system is able to visualize interactively the patient-specific models and their current relative position and alignment (Fig. 7).

For both shoulders, the motion limitations of eight different prosthesis types and sizes were measured. The prosthesis configurations were chosen so that a diverse set of impingement occurrences were observed. Any occurrence of impingement during motion tracking was specifically noted in the motion-tracking logs (Fig. 8). All motions were recorded as a time series of transformation matrices, tagged with prosthesis type and measurement information and then exported to a database.

The motions consisted of arm movement from 0° to maximum anteflexion, from 0° to maximum abduction, and finally from maximum exorotation to maximum endorotation at maximal elevation in the scapular plane. Occasionally, the motion was limited by the presence of soft tissue but, when possible, bone impingement was forced and noted for later comparison with the ROM simulations. The orthopaedic surgeon performing the arm motion visually determined whether a limitation was caused by bone impingement or by soft tissue. To evaluate the repeatability of the motions, four of the measurements were recorded twice.

Both shoulders with base plates were CT scanned post-operatively, using the same protocols as for the pre-operative scans. These data were then segmented. To avoid artefacts as a result of scattering, the post-operative models were combined with the pre-operative models by manually overlaying them (Fig. 9). Thus accurate bone models that have the prosthesis base platforms installed were obtained. These models were loaded into the pre-operative

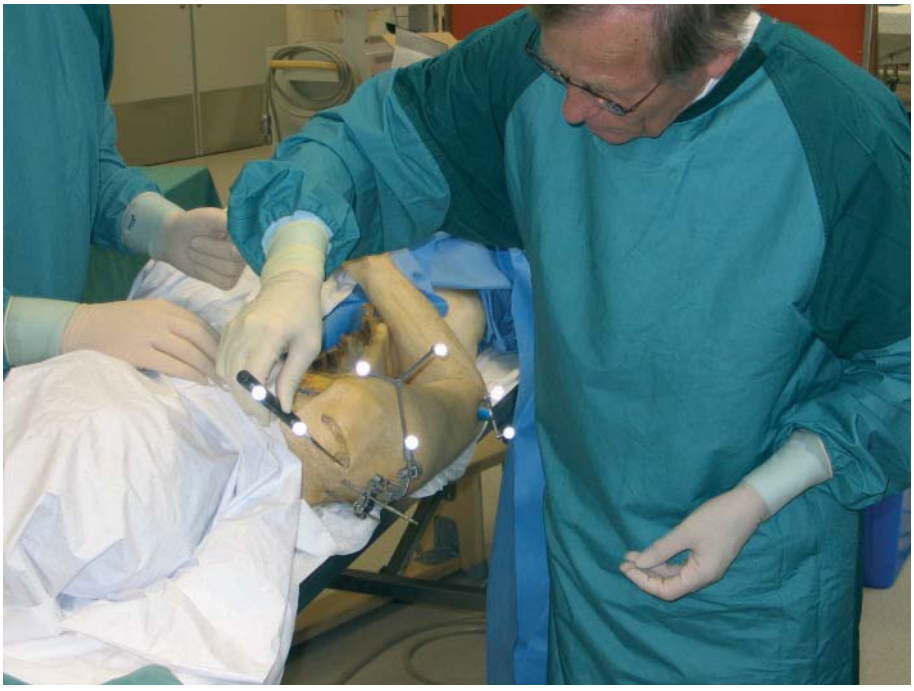

Fig. 6 After attachment of the marker tree, various landmarks on the scapula are indicated percutaneously. The markers on the sharp pointer, the scapula reference frame, and on the humeral tracker are visible

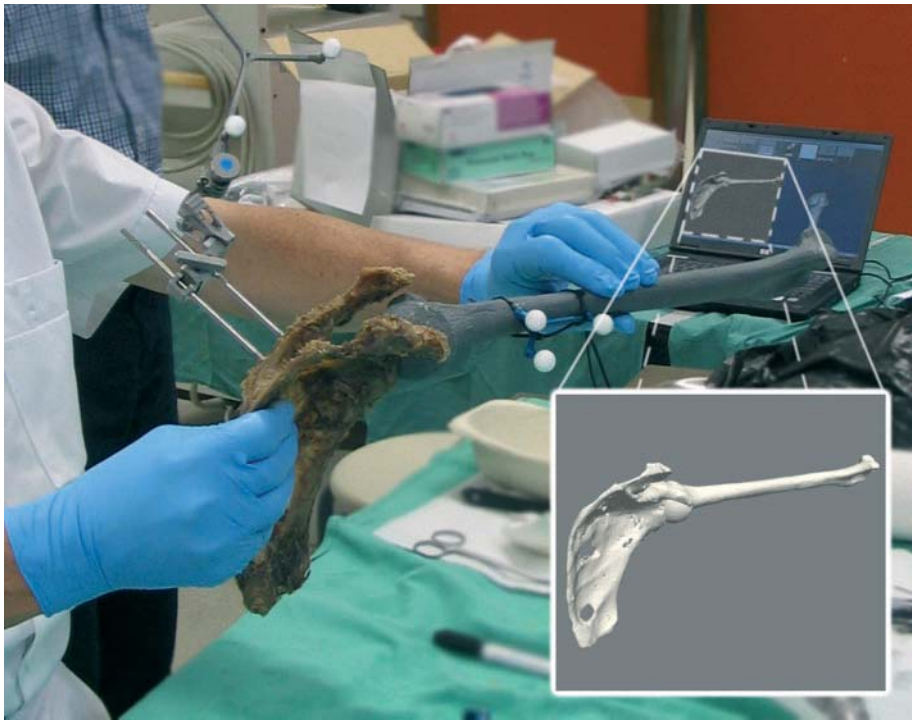

Fig. 7 Real-time motion tracking. Marker trees are attached to each bone, and these are tracked by the infrared guidance system. The intra-operative tracking system on the laptop shows the real-time position and orientation of the tracked bones

planning system. The motions were simulated by the ROM simulator of the pre-operative planning system and the resulting impingement angles were noted.

The advantage of using scanned post-operative models rather than virtually planning the operation is that the models used for the ROM simulations more accurately represent the geometry of the measured cadaver shoulders. Using the pre-operative planning functionality would introduce additional errors. It should be noted that the goal of this experiment is to validate the ROM simulations rather than the pre-operative planning system as a whole.

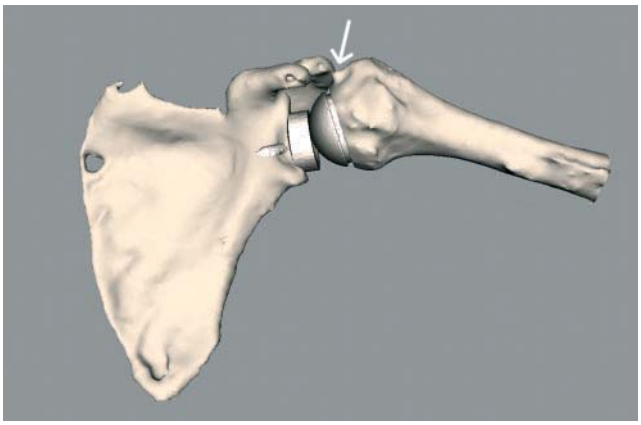

Fig. 8 Motion recording, showing impingement between the tuberculum majus on the humeral side and the acromion on the scapular side. The location of impingement is indicated by a white arrow

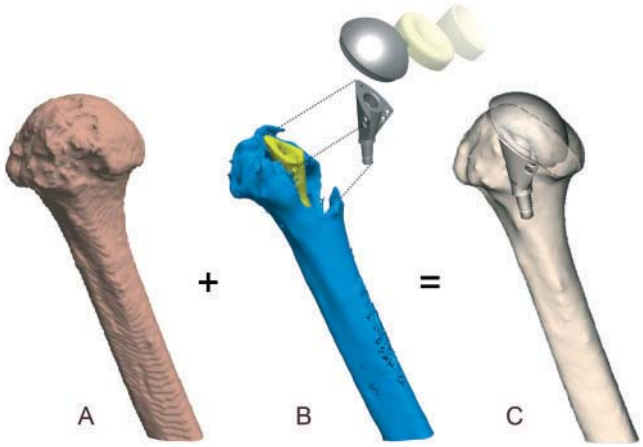

Fig. 9 Pre-operative surface model A and post-operative surface model B. Scattering caused by the prosthesis prevents complete segmentation of the CT data. However, by overlaying the two scans, the prosthesis position and alignment can be reconstructed to give C. The resulting models were used as input for the ROM simulations

The impingement angles as observed during the experiment were compared with the impingement angles as determined by the ROM simulator. The median deviation, the interquartile range, and maximum absolute deviation were calculated for the three separate motions as well as the complete set of measurements. For these calculations the measurements of the left shoulder and right shoulder were combined.

3 RESULTS

The ROM simulations and experimental observations are listed in Table 1. The observed limitations were sometimes caused by the fact that soft tissue was not capable of extending any further as a result of tension. These limitations are also given for reasons of completeness. The accuracy of the ROM simulations can be determined by examining the difference between the measurements of the cadaver experiment and the simulations. Motions that were recorded twice were very similar with almost identical motion limitations (difference, less than 0.5°) and are therefore not listed.

As Table 2 indicates, the observed impingement angles of the cadaver experiment correspond to the impingement predictions of the system. The median deviation is limited to a few degrees for all motions. To determine the statistical significance the Spearman rank correlation coefficient was calculated, resulting in a correlation of 0.982 with a significance of $p < 0.005$.

The ROM of the left shoulder differed from the ROM of the right shoulder owing to the different alignment of the base platforms. For both shoulders, impingement was observed more frequently for reverse prostheses than for normal prostheses. Impingement with the upper structures of the scapula (the acromium and coracoid process) occurred frequently during anteflexion and abduction, because of the more medial location of the centre of rotation. In addition, scapular notching was seen for almost all motion recordings of reverse prosthesis configurations.

Table 1 Results of the motion recordings and ROM simulations for both shoulders. The ball and cup prosthesis components have a radius of 22 mm. If applicable, the h value gives the height of the component at its centre-line. Because the simulator does not take into account soft tissue, bone impingement occurs for all motions. This is in contrast with the results of the cadaver observations, where the ROM was also occasionally limited by soft tissue. When a value is printed in italics, this means that the motion limitation was caused by soft tissue. Motion limitations that were not measured during the experiment are indicated by the word No. To facilitate comparison, the observed impingement angles are printed in bold, together with their simulated counterparts

Prosthesis configuration			Left shoulder				Right shoulder			
			Simulated impingement		Observed limitation		Simulated impingement		Observed limitation	
Humeral insert	Glenoid insert	Motion	Begin	End	Begin	End	Begin	End	Begin	End
Ball ($h = 14$ mm)	Cup	Abduction	0	84	No	*63.5*	−6	56	No	*52.9*
		Endorotation	−28	**71**	*16.6*	**69.2**	**−3.3**	**94**	**−5.5**	**95.7**
		Anteflexion	0	90	No	*61.6*	−33	112	No	*42.1*
Ball ($h = 18$ mm)	Cup	Abduction	0	91	No	*62.7*	−6	56	No	*52.8*
		Endorotation	−27	**72**	*27.3*	**69.6**	−43	**101**	*−3.2*	**98.6**
		Anteflexion	0	87	No	*67.5*	−35	111	No	*43.2*
Ball ($h = 14$ mm) eccentric	Cup	Abduction	2	85	No	*64.5*	−4	54	No	*52.7*
		Endorotation	−16	**52**	*16.4*	**59.1**	−18	**105**	*9.7*	**111.8**
		Anteflexion	4	**79**	No	**70.7**	−30	112	No	*41.0*
Ball ($h = 18$ mm) eccentric	Cup	Abduction	3	84	No	*56.2*	−5	53	No	*49.5*
		Endorotation	−13	**39**	*6.5*	**42.8**	−39	**94**	*13.7*	**96.0**
		Anteflexion	3	82	No	*66.1*	−28	112	No	*36.6*
Cup eccentric	Ball ($h = 14$ mm)	Abduction	21	**75**	No	**72.5**	7	**49**	No	**55.3**
		Endorotation	**16**	**69**	**11.6**	**71.5**	**−8**	**63**	**−6.5**	**62.2**
		Anteflexion	17	**56**	No	**62.7**	7	88	No	*37.2*
Cup proximal slope	Ball ($h = 14$ mm)	Abduction	19	**71**	No	**68.5**	**7**	**47**	**6.1**	**46.1**
		Endorotation	**−5**	**44**	**−2.2**	**48.9**	**−10**	**63**	**−6.9**	**67.4**
		Anteflexion	**23**	**61**	**25.1**	**58.8**	**7**	55	**10.4**	*41.0*
Cup anterior slope	Ball ($h = 14$ mm)	Abduction	18	**68**	No	**68.3**	**11**	**50**	**10.0**	**52.6**
		Endorotation	**18**	**70**	**15.0**	**72.1**	−14	**46**	*−2.9*	**49.9**
		Anteflexion	23	**61**	No	**60.0**	**18**	66	**19.5**	*36.4*
Cup distal slope	Ball ($h = 14$ mm)	Abduction	**33**	**73**	**31.5**	**68.4**	**26**	**51**	**26.2**	**49.7**
		Endorotation	**−1**	**57**	**−2.6**	**63.9**	−7	**63**	*−9.2*	**70.8**
		Anteflexion	28	59	No	*56.9*	**26**	75	**25.7**	*39.3*

Table 2 Summary of the results presented in Table 1. The accuracy of the ROM simulator is determined by comparing the impingement angles of the simulator with the observed occurrences of impingement. For these statistics, the motion limitations of the left shoulder and right shoulder were grouped. Only the measurements where bone impingement was observed are included

Motion	Median deviation (deg)	Interquartile range (deg)	Maximum absolute deviation (deg)
Abduction	0.95	2.53 (−0.28–2.25)	7.25
Endorotation	−2.10	6.20 (−4.40–1.80)	6.50
Anteflexion	−0.60	4.98 (−3.08–1.90)	8.90
All	−0.30	5.20 (−3.40–1.80)	8.60

Inaccuracy as a result of the hardware limitations of the BrainLAB VectorVision system was also determined during this experiment [**20**]. The mean translational error for locating a marker was 0.1 mm, 0.05 mm, and 0.25 mm in the *x*, *y*, and *z* directions respectively. Because the scapula and humerus marker trees are approximately 30 cm apart, the maximal angular error introduced by hardware limitations is smaller than 0.1°. This error is acceptable for the experiment.

To determine how accurately the post-operative models were overlaid with the pre-operative models, the minimum distances between the models were calculated on a per-vertex base. Because the post-operative models were different near the replaced regions, only a clipped half of each of the models was used. The mean error was 0.41 mm with a standard deviation of 0.23 mm. Increasing the accuracy of the models does not lead to substantially different ROM simulation results.

4 DISCUSSION

In this paper an experiment for the evaluation of the accuracy of the ROM simulation module was described. A CT-based navigation system, with which passive cadaveric joint motion was tracked, was developed. Subsequently, the recorded motions were compared with ROM simulations in order to validate the latter.

Reports have been given in the literature on the use of ROM simulations and impingement prediction for total hip replacement procedures. Jaramaz *et al.* [**21**] and Yoshimine *et al.* [**22**] analytically determined ROM as imposed by the prosthesis geometry. Sato *et al.* [**23**] studied the advantages of impingement prediction for the hip joint, using both the prosthesis geometry and the surface data of the bone. Their simulations were also clinically validated using optical tracking. To the present authors' knowledge, no publications exist describing validated simulation of bone-determined ROM for shoulder replacement surgery, even though the occurrence of impingement complications after shoulder replacement surgery is a frequently seen problem.

There are limitations to this study. The number of two shoulders is relatively low to make claims on the accuracy of the ROM simulator. However, the utilization of different prosthesis configurations leads to a larger number of unique impingement cases that can be used for validation of the ROM simulator.

Optical tracking systems are known to have some inaccuracy owing to the registration step, which requires the surgeon to indicate the exact same points on the physical bones as on the virtual bones. Differences between these locations result in a registration error. However, for the measurements in this experiment, only the rotational information as provided by the optical tracking system was used. This information relies on the relative movement of the marker trees rather than absolute positions. If registered landmarks are close to each other, this may introduce a small error in the rotation axis. Because the medial and lateral epicondyles are relatively close to one another, it is expected that a small registration error will have been introduced in the axis used for endorotation. On the basis of visual inspection of the registration it is suspected that this error was limited. However, for definition of the axes used to measure abduction and anteflexion the selected landmarks are sufficiently far apart. In future a possible solution to this problem is the utilization of fiducial markers that are inserted before acquisition of the pre-operative CT scan and can later be used to ensure a correct registration.

The ROM simulator uses CT data as acquired by the standard scanning protocol for shoulders. However, the time required to segment the data manually is approximately 1 h. This may complicate clinical applicability of the system. The present authors are currently working on new techniques and algorithms to speed up this segmentation process.

From the results it is concluded that the impingement predictions of the system generally correspond

to the actual incidence of impingement during recorded shoulder motion. However, a number of observed ROMs were smaller than their simulated counterparts. This was expected and can be explained by the movement restrictions as imposed by the presence of soft tissue. Because soft tissue is not incorporated into the ROM simulations, the simulations are restricted to predict motion limitations as imposed by bony impingement. This already is quite helpful to the surgeon, as it alerts the surgeon to possible impingement complications.

The simulations confirm that the humeral component of a reverse prosthesis frequently impinges on either the glenoid component or the glenoid. As discussed in the introduction, this may cause early loosening of the glenoid prosthesis and leads to bone damage, further complicating revision surgery. Subacromial and subcoracoid impingement was also observed for most of the total reverse shoulder configurations. The accuracy of the ROM simulations is well within the range to predict these impingement complications beforehand, allowing the surgeon to adapt the pre-operative plan.

Future work will include the implementation of an intra-operative guidance system, based on the optical tracking system described in this paper. The intra-operative guidance system will ensure that the actual surgery corresponds to the pre-operative plan as defined by the surgeon with the pre-operative planning system.

If surgery is conducted according to the pre-operative plan as composed in the pre-operative planning system, it is plausible that the post-operative bone-determined ROM corresponds to the ROM as predicted pre-operatively by this system. Moreover, all the observed occurrences of impingement during the described experiment were predicted by the system. Therefore it is recommended that the ROM predictions of the system during the planning stage of a shoulder replacement procedure are complied with, keeping in mind other aspects such as prosthesis fixation and the presence of soft tissue. Finally, from the results of this experiment it is concluded that the system is particularly useful for non-anatomical prosthetic designs such as reverse prostheses, because they entail an increased risk of impingement complications.

ACKNOWLEDGEMENTS

This work was supported by a grant from the Dutch Rheumatism Foundation (Reumafonds). The present authors thank the Radiology and Anatomy Departments of the Leiden University Medical Centre for their assistence in performing this research. Finally, thanks are due to BrainLAB AG for making available a navigation system, and to Zimmer Inc for the use of their cadaver instrument set.

REFERENCES

1 **Hasan, S. S., Leith, J. M., Smith, K. L.,** and **Matsen III, F. A.** The distribution of shoulder replacements among surgeons is significantly different than that of hip or knee replacement. *J. Shoulder Elbow Surg.*, 2003, **12**(2), 164–169.

2 **Hasan, S. S., Leith, J. M., Campbell, B., Kapil, R., Smith, K. L.,** and **Matsen III, F. A.** Characteristics of unsatisfactory shoulder arthroplasties. *J. Shoulder Elbow Surg.*, 2002, **11**(5), 431–441.

3 **Iannotti, J. P., Spencer Jr, E. E., Winter, U., Deffenbaugh, D.,** and **Williams, G.** Prosthetic positioning in total shoulder arthroplasty. *J. Shoulder Elbow Surg.*, 2005, **14**(1 Suppl. 1), S111–S121.

4 **Dines, D. M., Warren, R. F.,** and **Rodriguez, D. F.** Revision shoulder arthroplasty. *Techqs Shoulder Elbow Surg.*, 2001, **2**, 26–37.

5 **Williams Jr, G. R., Wong, K. L., Pepe, M. D., Tan, V., Silverberg, D., Ramsey, M. L., Karduna, A.,** and **Iannotti, J. P.** The effect of articular malposition after total shoulder arthroplasty on glenohumeral translations, range of motion, and subacromial impingement. *J. Shoulder Elbow Surg.*, 2001, **10**(5), 399–409.

6 **Grammont, P. M., Trouilloud, P., Laffay, J. P.,** and **Deries, X.** Etude et réalisation d'une nouvelle prothèse d'épaule. *Rhumatologie*, 1987, **39**, 407–418.

7 **Guery, J., Favard, L., Sirveaux, F., Oudet, D., Mole, D.,** and **Walch, G.** Reverse total shoulder arthroplasty: survivorship analysis of eighty replacements followed for five to ten years. *J. Bone Jt Surg. Am.*, 2006, **88**(8), 1742–1747.

8 **Rockwood Jr, C. A.** The reverse total shoulder prosthesis. The new kid on the block. *J. Bone Jt Surg. Am.*, 2007, **89**(2), 233–235.

9 **Sirveaux, F., Favard, L., Oudet, D., Huquet, D., Walch, G.,** and **Mole, D.** Grammont inverted total shoulder arthroplasty in the treatment of glenohumeral osteoarthritis with massive rupture of the cuff: results of a multicentre study of 80 shoulders. *J. Bone Jt Surg. Br.*, 2004, **86**(3), 388–395.

10 **Juvenspan, M., Nourissat, G.,** and **Doursounian, L.** La prothèse inversée depaule dans les ruptures massives et irréparables de la coiffe des rotateurs. *Maîtrise Orthopédique*, October 2005, **148**.

11 **Frankle, M., Siegal, S., Pupello, D., Saleem, A., Mighell, M.,** and **Vasey, M.** The reverse shoulder prosthesis for glenohumeral arthritis associated with severe rotator cuff deficiency. A minimum two-year follow-up study of sixty patients. *J. Bone Jt Surg. Am.*, 2005, **87**(8), 1697–1705.

12 **Nyffeler, R. W., Werner, C. M. L.,** and **Gerber, C.** Biomechanical relevance of glenoid component positioning in the reverse Delta III total shoulder prosthesis. *J. Shoulder Elbow Surg.*, 2005, **14**(5), 524–528.

13 **Simovitch, R. W., Zumstein, M. A., Lohri, E., Helmy, N.,** and **Gerber, C.** Predictors of scapular notching in patients managed with the Delta III reverse total shoulder replacement. *J. Bone Jt Surg. Am.*, 2007, **89**(3), 588–600.

14 **Krekel, P. R., Botha, C. P., Valstar, E. R., de Bruin, P. W., Rozing, P. M.,** and **Post, F. H.** Interactive simulation and comparative visualisation of the bone-determined range of motion of the human shoulder. In *Simulation und visualisierung 2006 (SimVis 2006)* (Eds T. Schulze, G. Horton, B. Preim, and S. Schlechtweg), Magdeburg, Germany, 2–3 March 2006, pp. 275–288 (SCS Publishing House, Erlangen).

15 **van der Glas, M., Vos, F. M., Botha, C. P.,** and **Vossepoel, A. M.** Determination of position and radius of ball joints. In *Medical imaging 2002: image processing*, Proceedings of SPIE, vol. 4684, 2002, pp. 1571–1577 (SPIE, Bellingham, Washington).

16 **Meskers, C. G. M., van der Helm, F. C. T., Rozendaal, L. A.,** and **Rozing, P. M.** *In vivo* estimation of the glenohumeral joint rotation center from scapular bony landmarks by linear regression. *J. Biomechanics*, 1998, **31**(1), 93–96.

17 **Wu, G., Van der Helm, F. C. T., Veeger, H. E. J., Makhsous, M., Van Roy, P., Anglin, C., Nagels, J., Karduna, A. R., McQuade, K., Wang, X., Werner, F. W.,** and **Buchholz, B.** ISB recommendation on definitions of joint coordinate systems of various joints for the reporting of human joint motion – part II: shoulder, elbow, wrist and hand. *J. Biomechanics*, 2005, **38**(5), 987–992.

18 **Terdiman, P.** Memory-optimized bounding-volume hierarchies, 2001, available from http://www.codercorner.com/Opcode.htm.

19 **Botha, C. P.** *Techniques and software architectures for medical visualisation and image processing*. PhD Thesis, Delft University of Technology, Delft, The Netherlands, 2005.

20 **de Bruin, P. W., Krekel, P. R., Valstar, E. R.,** and **Rozing, P. M.** Bony landmark registration for computer navigation of the shoulder: evaluation of accuracy. In Proceedings of the Seventh Annual Meeting of International Society for Computer Assisted Orthopaedic Surgery (*CAOS 2007*), Heidelberg, Germany, 20–23 June 2007, pp. 746–748 (Pro Business, Berlin).

21 **Jaramaz, B., Nikou, C., Simon, D. A.,** and **Di Gioia, A. M.** Range of motion after total hip arthroplasty: experimental verification of the analytical simulator. Technical Report CMU-RI-TR-97-09, Robotics Institute, Carnegie Mellon University, Pittsburgh, Pennsylvania, USA, February 1997.

22 **Yoshimine, F.** and **Ginbayashi, K.** A mathematical formula to calculate the theoretical range of motion for total hip replacement. *J. Biomechanics*, 2002, **35**(7), 989–993.

23 **Sato, Y., Sasama, T., Sugano, N., Nakahodo, K., Nishii, T., Ozono, K., Yonenobu, K., Ochi, T.,** and **Tamura, S.** Intraoperative simulation and planning using a combined acetabular and femoral (CAF) navigation system for total hip replacement. In *Medical image computing and computer-assisted intervention (MICCAI 2000)*, Lecture Notes in Computer Science, vol. 1935, 2000, pp. 1114–1125 (Springer-Verlag, Berlin).